Laser ionization based on resonance saturation—a simple model description

R. M. Measures and P. G. Cardinal
Institute for Aerospace Studies, University of Toronto, 4925 Dufferin Street, Downsview, Ontario M3H 5T6, Canada
(Received 21 March 1980)

We have developed a simple physical model of *laser ionization based on resonance saturation* that involves the most important collisional and radiative interactions, yet lends itself to analytical solutions that enable the time history of the free electron density to be evaluated. We have been able to demonstrate that in the case of sodium the predictions of this simple model are within 15% of the values calculated by our extensive LIBORS computer code. The model has also been used to estimate the ionization time for each of the alkali metals over a wide range of conditions. These results are found to be consistent with several experimental observations.

INTRODUCTION

Laser-induced ionization is of considerable interest both from the standpoint of understanding the mechanisms involved and from attempts to exploit these interactions in a diverse range of applications. During the last few years there has grown a considerable body of experimental evidence to indicate that intense illumination of a resonance transition of an atomic vapor in the density range (10^{13}–10^{17} cm^{-3}) leads to substantial excitation and ionization.[1-8] Indeed, the degree of ionization achieved has been found to approach 100% if the duration of the laser pulse greatly exceeds the lifetime of the resonance state.[1-3]

Although at low densities (below 10^{13} cm^{-3}) multiphoton processes tend to dominate the ionization, for densities above 10^{13} cm^{-3} collisional effects start to play an important role and significant levels of excitation and ionization can be achieved for quite low values of laser irradiance.[6-8] Lucatorto and McIlrath[1,2] were the first to demonstrate that if laser radiation of relatively modest power density (~10^{6} $W\,cm^{-2}$) were tuned to the resonance line of an alkali metal vapor (density 10^{15}–10^{16} cm^{-3}), almost complete ionization resulted in a remarkably short period—far shorter than could be accounted for in terms of any multiphoton or atom-atom collisional process.[9] The validity of these results has been substantiated by similar experimental work of Skinner[3] and Young *et al.*[4] The explanation for this efficient and rapid new method of ionization can be found in a much earlier paper devoted to laser enhancement of ionization for MHD power generation.[10] In that paper one of the present authors had proposed that under conditions of laser saturation of a resonance transition, the energy of any free electrons would be rapidly increased by superelastic collision quenching of the overpopulated resonance level. Subsequently, the rate of ionization would be dramatically enhanced, not only as a result of the increased electron temperature, but also by virtue of the fact that the laser-maintained resonance-state population constitutes a substantial pool of atoms (roughly $\frac{1}{2}$) having an ionization energy that is reduced by the laser-photon energy.

In experiments where there is essentially no initial ionization, multiphoton ionization,[9,11] laser-induced Penning ionization,[9] or associative ionization[12] could liberate the "seed" electrons required for the above mechanism. Although associative ionization has been found to have very large cross sections for high-lying Rydberg states,[13] an effective value of around 10^{-17} cm^{2} seems to be more appropriate[12,14] for alkali resonance transitions. In spite of this small cross section, Cardinal[15] has shown that associative ionization would dominate the initial-rate of ionization in the experimental work with sodium of Lucatorto and McIlrath.[1,2]

We have developed a fairly comprehensive code for studying laser ionization based on resonance saturation (LIBORS). This code treats the laser-excited atom as a 20-energy-level system and solves the subsequent set of energy and population rate equations by a fourth-order Runge-Kutta technique. A detailed description of the code is presented elsewhere[15-18] and will not be repeated here. It will suffice to mention that the code evaluates the temporal behavior of (i) each of the 20-atomic-level populations, (ii) the free electron density, (iii) the free electron temperature, (iv) the ion and neutral temperatures, (v) the laser power absorbed per unit volume, and (vi) the power radiated per second per unit volume as a result of radiative recombination to the resonance level, assuming a steplike laser pulse.

The results of our computer simulations for sodium are consistent with the experimental observations of Lucatorto and McIlrath[1] and suggest that LIBORS might be ideal for creating the plasma guide channels that are deemed to be

necessary for transportation of electron or ion beams to the fuel pellet of future particle-beam fusion reactors.[17] We have also shown that the concepts of *superelastic laser-energy conversion* (SELEC) could, under certain conditions, have several advantages over inverse bremsstrahlung as a means of coupling laser energy into a plasma or an un-ionized gaseous medium. In the event that SELEC is applied to a strong transition within a suitable ionic species, extremely rapid rates of plasma heating can be achieved[19]—a feature that is quite conducive to the development of short-wavelength lasers. Indeed, in the case of a boron III plasma, we predict[19] that a heating rate in excess of 10^{13} K sec^{-1} could be attained with a laser irradiance of close to 10^8 W cm^{-2}.

The purpose of the present paper is to reveal a relatively simple physical model of LIBORS that lends itself to an analytical expression for the temporal growth of ionization, yet retains almost all of the important interactions. This model allows us to predict the ionization time under a wide range of conditions and is very helpful in providing a physical interpretation of the more comprehensive LIBORS code results. Of particular significance is the fact that this simple model enables us to quickly and inexpensively extend our ionization time estimates to other elements. Several examples are provided which are found to be consistent with experimental observations. In the case of solium our simple-model ionization-time predictions have been found to agree to within 15% of our full LIBORS code results.

In passing, we feel obliged to comment on the term saturation, as used in the above context. Recently, some confusion has been displayed in the literature[20-22] regarding the attainment and meaning of saturation. In particular, several workers have suggested that their experiments have failed to demonstrate saturation of the laser-induced fluorescence (or intensified spontaneous emission) even at high values of laser irradiance. In the context of the present paper, saturation is taken to mean that the resonance to ground-level population densities are locked in the ratio of their degeneracies by the laser fields. This concept was first enunciated by Measures.[23] Recently, Salter *et al.*[24] have demonstrated that this condition can in fact apply, even though the laser-induced fluorescence fails to saturate at the corresponding laser irradiance. Salter[22] has attributed this failure to observe saturation to radiation trapping. However, Rodrigo and Measures[25] and Daily[26] have provided an alternative explanation of this effect in terms of the laser beam's radial profile and the spatially averaged signal. Some combination of these mechanisms might in fact be needed to adequately account for this anomalous observation.

LIBORS SIMPLE-MODEL FORMULATION

We shall consider the case of a homogeneous, single-constituent, atomic gaseous medium suddenly irradiated with an intense pulse of laser radiation that is tuned to one of the electronic resonance transitions. Although the interaction of this radiation field with the atoms is most accurately treated through use of the density-matrix approach, a rate equation analysis is reasonably reliable[27] if the bandwidth of the laser radiation is large compared to the Rabi frequency $|\Omega_r|$. In the case of a strong transition, $|\Omega_r| \approx 10^8\sqrt{I'}$ rad sec^{-1}, where I' W cm^{-2} is the frequency-averaged laser irradiance, and a rate equation analysis will be reasonable for most laser-ionization experiments (where the typical laser line width $\gtrsim 0.05$ nm) up to a laser irradiance of about 10^8 W cm^{-2}.

Rapid collisional dephasing also improves the reliability of the rate equation analysis. Under conditions of resonance collisional broadening, the dephasing time can be less than, or of the order of, 1 nsec for the densities of interest according to McIlrath and Carlsten.[28]

The model we shall develop is particularly appropriate to atoms with low-lying resonance states, such as the alkali metals. For this class of atoms, $2E_{21} < E_{c1} \lesssim 3E_{21}$, where E_{21} represents the energy difference between the ground and the laser-excited resonance state (and is consequently equal to the laser-photon energy $h\nu$) and E_{c1} represents the ionization energy of the ground state. If the laser radiation is assumed to be suddenly applied at $t=0$, then the subsequent chain of events can be viewed as proceeding in the four stages indicated in Fig. 1.

According to Measures[23] the resonance to ground-state population densities are locked in the ratio of their degeneracies, *viz.*, $N_2/N_1 \approx g_2/g_1 \equiv g$, in a characteristic time $\tau_R \approx [(1+g)R_{21}]^{-1}$, provided $I'(\nu) \gg I_s(\nu)$ in the case of broadband laser radiation. $R_{21}[\equiv B_{21}\int I'(\nu)\mathfrak{L}(\nu)d\nu/4\pi]$ represents the stimulated emission-rate coefficient for the resonance transition. B_{21} represents the appropriate Milne coefficient and $\mathfrak{L}(\nu)$ the corresponding line-profile function. $I'(\nu)$ represents the laser spectral irradiance and $I_s(\nu)$ is the saturated spectral irradiance, given by

$$I_s(\nu) = \frac{8\pi h\nu^3}{c^2(1+g)}\left(\frac{\tau_2^{\mathrm{RAD}}}{\tau_2}\right),$$

where $\tau_2^{\mathrm{RAD}}(\equiv A_{21}^{-1})$ and τ_2 is the resonance-state lifetime. A_{21} is the resonance transition Einstein

probability. Invariably, τ_R is very short (much less than 1 nsec for the typical laser fields under consideration) compared to any other process and we assign laser saturation to stage 1.

Once the large pool of resonance-state atoms is created, several kinds of interactions give rise to a linear growth of the free-electron density associated with stage 2. The most important of these are

(i) two-photon ionization of the resonance level:

$$A^* + 2h\nu \rightarrow A^+ + e + \mathrm{KE}\ ,$$

(ii) laser-induced Penning ionization:

$$A^* + A^* + h\nu \rightarrow A + A^+ + e + \mathrm{KE}\ ,$$

and

(iii) associative ionization:

$$A^* + A^* \rightarrow A_2^+ + e + \mathrm{KE}\ .$$

A^* represents a laser-excited resonance-state atom, A^+ the ionic species, and A a ground-state atom of the same species. A_2^+ represents the dimer ion. In the case of the alkali metals, Geltman,[9] de Jong and van der Valk,[12] and Klucharev *et al.*[14] have provided the relevant cross sections. The appropriate rate of ionization during stage 2 can be expressed in the form

$$\left.\frac{dN_e}{dt}\right|_{\text{stage 2}} \approx N_2\sigma_{2c}^{(2)}F^2 + \tfrac{1}{2}N_2^2\sigma_L v F + \tfrac{1}{2}N_2^2\sigma_A v\ , \qquad (1)$$

where $\sigma_{2c}^{(2)}$ (cm^4 sec) is the two-photon, resonance-state, ionization-rate coefficient, σ_L (cm^4 sec) is the laser-induced Penning ionization-rate coefficient, σ_A (cm^2) is the effective associative ionization cross section (allowing for the energy defect of the interaction[14]), v (cm sec^{-1}) is the mean atom velocity, and F (photons cm^{-2} sec^{-1}) represents the laser photon flux density, i.e., $F = \int I^1(\nu)d\nu/h\nu$.

The electrons created by these initial processes rapidly gain energy through superelastic collision quenching of the laser sustained resonance-state population, as first suggested by Measures.[10]

In stage 3, the free-electron temperature[29] is viewed as stabilizing as a result of a balance between the rate of superelastic heating and excitation cooling. This will be considered in more detail later. These electrons now give rise to an exponential growth in the free-electron density due to both direct collisional ionization of the resonance level and single photon-laser ionization of the collisionally populated intermediate levels.

Finally, in stage 4, runaway collisional ionization of the intermediate levels occurs once a critical electron density is achieved. This process leads to the ionization burnout that results in almost complete ionization of the laser pumped species. Our full LIBORS computer code[15,18] indicates that during this rapid burnout phase, superelastic

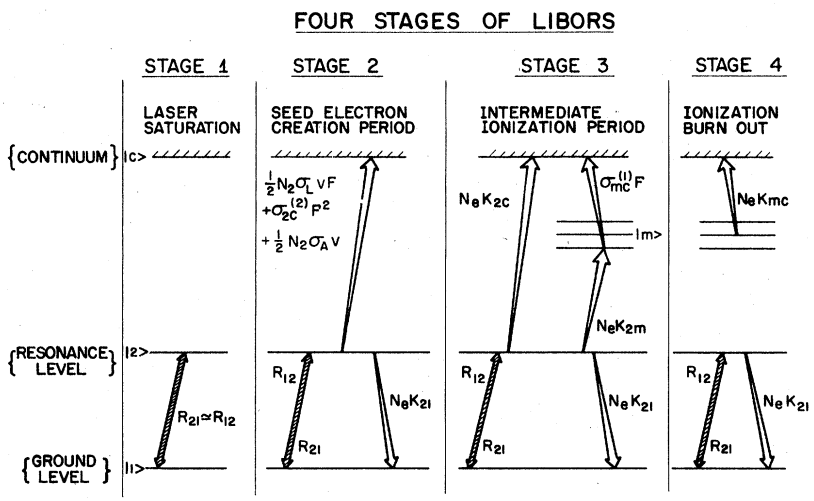

FIG. 1. Four stages of LIBORS. Stage 1: Laser rapidly locks ground and resonance-level populations in ratio of degeneracies. Stage 2: (i) Rapid growth of free electrons due to two-photon ionization of resonance level and laser-induced Penning ionization. Associative ionization is important for some elements. (ii) Free electrons rapidly gain energy through superelastic collisions. Stage 3: (i) Direct electron-impact ionization of resonance level and single-photon ionization of collisionally populated upper levels dominate the rate of ionization. (ii) Electron temperature stabilizes as the rate of superelastic heating balances rate of collisional cooling through excitation. Stage 4: (i) Runaway collisional ionization of upper levels occurs once a critical electron density is achieved. (ii) Superelastic heating can no longer balance collisional cooling and the electron temperature falls.

heating is unable to maintain the free-electron temperature and a sudden drop in the temperature is expected.

In order to obtain an analytical solution for the ionization time from our LIBORS simple model, we shall assume that the free-electron temperature stabilizes and remains constant throughout both stages 3 and 4. Some justification for this assumption can be found in the following argument. During the linear growth period (stage 2), the dominant ionization processes are independent of the free-electron temperature. This is fortunate because it is questionable whether the electron energy distribution could be characterized by a temperature during this period.[29]

The appropriate energy equation for the free electrons takes the form

$$\frac{d}{dt}(N_e\epsilon_e)=N_2N_eK_{21}E_{21}+(2E_{21}-E_{c2})N_2\sigma_{2c}^{(2)}F^2+\sum_{m>m^*}(E_{21}-E_{cm})N_m\sigma_{mc}^{(1)}F$$
$$+\tfrac{1}{2}(2E_{21}-E_{c2})N_2^2\sigma_L vF+\tfrac{1}{2}(2E_{21}-E_A)N_2^2\sigma_A v-N_e\sum_{m\geq 1}N_mK_{mc}E_{cm}$$
$$-N_eC-N_e^2H_{ei}-N_eN_aH_{ea}+N_e^3\sum_{m\geq 1}K_{cm}E_{cm}-N_e^2\epsilon_e\sum_{m\geq 1}\beta(m)\,, \tag{2}$$

where $\epsilon_e(J)$ represents the mean translation energy of a free electron, K_{mn} ($\mathrm{cm^3\,sec^{-1}}$) represents the rate coefficient for an electron collision induced transition from level m to n,[15] K_{mc} ($\mathrm{cm^3\,sec^{-1}}$) represents the rate coefficient for an electron collision induced ionization transition from level m,[15] K_{cm} ($\mathrm{cm^6\,sec^{-1}}$) represents the three-body recombination coefficient,[15] $\sigma_{mc}^{(2)}$ ($\mathrm{cm^2}$) represents the single-photon ionization cross section[30] for level m, and the sum extends over all levels $m>m^*$ for which ionization by a single laser photon can be achieved, N_m ($\mathrm{cm^{-3}}$) represents the number density of atoms in the m energy state, C represents the loss of energy per electron due to the net collisionally induced upward movement of bound electrons (exclusive of the resonance superelastic term)

$$C=\sum_{n\geq 1}\sum_{m>n}(N_nK_{nm}-N_mK_{mn})E_{mn}-N_2K_{21}E_{21}\,, \tag{3}$$

E_{mn} (J) represents the energy separation between levels m and n, E_{cn} (J) represents the ionization energy of level n, E_A (J) represents the energy required for the associative ionization of two laser-excited atoms, H_{ei} ($\mathrm{J\,cm^3\,sec^{-1}}$) represents the rate of elastic energy transfer to ions through Coulomb scattering collisions,[17] N_a ($\mathrm{cm^{-3}}$) represents the total neutral atom density, H_{ea} ($\mathrm{J\,cm^3\,sec^{-1}}$) represents the rate of elastic energy coupling between the free electrons and the neutral atoms.[17] β ($\mathrm{cm^3\,sec^{-1}}$) represents the rate of radiative recombination to level m. Equation (2) can be divided into two equations, one for the rate of growth of the free electron density

$$\tfrac{3}{2}kT_e\frac{dN_e}{dt}=\tfrac{3}{2}kT_e\left(N_2\sigma_{2c}^{(2)}F^2+\tfrac{1}{2}N_2^2v(\sigma_A+\sigma_L F)+\sum_{m>m^*}N_m\sigma_{mc}^{(1)}F+N_e\sum_{m\geq 1}N_mK_{mc}-N_e^2\sum_{m\geq 1}[N_eK_{cm}+\beta(m)]\right), \tag{4}$$

where T_e (K) represents the free-electron temperature (*viz.*, $\epsilon_e=\frac{3}{2}kT_e$), and the other for the variation of the free-electron temperature,

$$N_e\frac{d}{dt}(\tfrac{3}{2}kT_e)=N_eN_2K_{21}E_{21}+(2E_{21}-E_{c2}-\tfrac{3}{2}kT_e)(N_2\sigma_{2c}^{(2)}F^2+\tfrac{1}{2}N_2^2\sigma_L vF)$$
$$+\tfrac{1}{2}(2E_{21}-E_A-\tfrac{3}{2}kT_e)N_2^2\sigma_A v+N_e^3\sum_{m\geq 1}K_{cm}(E_{cm}+\tfrac{3}{2}kT_e)$$
$$-N_e\sum_{m\geq 1}N_mK_{mc}(E_{cm}+\tfrac{3}{2}kT_e)+\sum_{m>m^*}(E_{21}-E_{cm}-\tfrac{3}{2}kT_e)N_m\sigma_{mc}^{(1)}F-N_eC-N_e^2H_{ei}-N_eN_aH_{ea}\,. \tag{5}$$

Considerable simplification of these equations can be achieved if we restrict our time of interest to the interval for which the degree of ionization is less than a few percent. This will incur only a small loss of accuracy in predicting the ionization time as the ionization proceeds from a few percent to almost total ionization in a very small fraction of the total time for full ionization, due to the very fast rate of ionization achieved in stage 4—the runaway region—a result confirmed

by our LIBORS code which does not make these simplifications.

Under these conditions we can write for the alkali metal vapors, where $2E_{21} < E_{c1} < 3E_{21}$, the rate of ionization in the form

$$\frac{dN_e}{dt} \simeq N_2[\sigma_{2c}^{(2)}F^2 + \tfrac{1}{2}N_2 v(\sigma_A + \sigma_L F) + N_e K_{2c}] + \sum_{m\geq 3} N_m(\sigma_{mc}^{(1)}F + N_e K_{mc}) . \quad (6)$$

The first term on the right-hand side of Eq. (5) represents the superelastic heating rate and it is possible to show that for times $\gtrsim \Delta E/(N_2 K_{21} E_{21})$, where $\Delta E \equiv 2E_{21} - E_{c2} - \frac{3}{2}kT_e$, this superelastic heating term will dominate the heating terms associated with the seed creation processes. For the alkali metals, this characteristic time is very short compared to the ionization time (at 10^{16} cm^{-3}, it is typically less than about 1 nsec). The gain in energy due to single-photon ionization and the loss in energy from direct-impact ionization of the resonance level are also neglected in comparison to the superelastic heating and excitation cooling terms in Eq. (5). Under these circumstances the free-electron energy equation, during stage 3 can be reasonably well expressed in the form

$$\frac{d}{dt}(\tfrac{3}{2}kT_e) \approx N_2 K_{21} E_{21} - N_1 K_{12} E_{21} - N_2 \sum_{m>2} K_{2m} E_{m2} . \quad (7)$$

The first term on the right-hand side of Eq. (7) represents the superelastic heating rate per electron, while the subsequent terms represent the cooling rate per electron associated with the dominant collisional excitation processes. The sum over m in the last term extends over the group of intermediate levels that are rapidly populated by *hot* electrons and depopulated by single-photon laser ionization.

Using electron collision-rate coefficients that are based upon Seaton cross sections,[31] Eq. (7) yields under conditions of laser saturation, a transcendental equation for the *steady-state superelastic temperature*,

$$T_e^s \approx \frac{E_{32}/k}{\ln\left(\exp(-\epsilon_1/kT_e^s) + g/\langle f_{12}\rangle \sum_{m\geq 3}\langle f_{2m}\rangle \exp(-\epsilon_m/kT_e^s)\right)} , \quad (8)$$

where $\epsilon_m \equiv E_{m2} - E_{32}$ and $\langle f_{im}\rangle \equiv f_{im}\langle \bar{G}\rangle_{im}$. f_{im} represents the absorption oscillator strength for the im transition and $\langle \bar{G}\rangle_{im}$ the relevant Gaunt factor averaged over a Maxwellian velocity distribution. This equation can be solved by an iterative procedure, or, in light of the logarithmic nature of the denominator and the fact that $E_{m2} \approx E_{32}$ (in the model), it can be approximated by the expression

$$T_e^s \approx \frac{E_{32}/k}{\ln\left(1 + g\sum_{m\geq 3}\frac{f_{2m}}{f_{12}}\right)} , \quad (9)$$

where we have also assumed $\langle \bar{G}\rangle_{im} \simeq 1$. This value of the free-electron temperature is then used to compute the various collision-rate coefficients.

The relevant intermediate-level population-rate equation can be expressed in the form

$$dN_m/dt = N_2 N_e K_{2m} - N_m(\sigma_{mc}^{(1)}F + A_m^{\dagger} + N_e K_m) , \quad (10)$$

where $A_m^{\dagger} = A_{ms}\gamma_{ms}$ represents the radiation-trapped Einstein transition probability for the ms transition, s can correspond to either the ground or resonance level, γ_{ms} is the Holstein escape factor,[32] and

$$K_m \equiv K_{mc} + \sum_{n\neq m} K_{mn} . \quad (11)$$

We have assumed that in light of the large population of the resonance-state atoms (due to laser saturation), $N_e N_2 K_{2m}$ will dominate any other rate of population of level m from other levels. This may not be strictly true for closely spaced adjacent levels, but such terms only serve to rapidly equilibrate the population within the manifold of intermediate states. If we introduce

$$P_m = \sigma_{mc}^{(1)}F \quad (12)$$

and set

$$\rho_m = P_m + A_m^{\dagger} , \quad (13)$$

then over a significant fraction of the ionization time

$$\rho_m \gg N_e K_m . \quad (14)$$

Under these circumstances, Eq. (10) has a solution of the form

$$N_m(t) = N_2 K_{2m} \exp(-\rho_m t)\int_0^t N_e(t^*)\exp(\rho_m t^*)dt^* \quad (15)$$

if the vapor is assumed to be unexcited prior to laser irradiation, i.e., $N_m(0) = 0$. F, N_2, and K_{2m} are also taken to be constant over the period of interest.

The constancy of N_2 over an appreciable fraction of the time to ionize is quite reasonable on the grounds that the upper levels ($m \geq 3$) only become significantly populated just prior to ionization burn-burnout (stage 4). In fact, if we use the saturation condition, we can write $N_2 \simeq GN_0$, where $G = g(1+g)^{-1}$ and N_0 represents the initial atom density. The time independence of K_{2m} is based upon our previous assumption of a stabilized temperature

during the intermediate phase (stage 3) and F has been set to be constant by our assertion of a step-like laser pulse. The viability of these assumptions will become apparent later when we review the LIBORS computer-code results.

It is apparent that substitution of Eq. (15) into the ionization equation yields a polynomial expansion in N_e on the right-hand side of Eq. (6). At the earliest times from the moment of laser saturation, i.e., stage 2, the free-electron-density growth rate is expected to be independent of N_e, while an exponential growth is to be expected during the subsequent period, stage 3. This suggests that a first approximation to the free-electron density can be expressed in the form

$$N_e(t) \simeq N_{e0}[\exp(\beta t) - 1]. \tag{16}$$

This gives a linear growth for $\beta t \ll 1$ and an exponential growth for $\beta t \gtrsim 1$. N_{e0} can be taken to be the seed electron density for which N_e departs significantly from a linear growth.

Substituting Eq. (16) into Eq. (15) yields

$$N_m(t) = \frac{N_2 K_{2m} N_e(t)}{\beta + \rho_m}\left[1 - \frac{\beta}{\rho_m}\left(\frac{1 - \exp(-\rho_m t)}{\exp(\beta t) - 1}\right)\right]. \tag{17}$$

For times sufficiently great for relaxation of the intermediate-level populations, we obtain an approximation relation of the form

$$N_m(t) \simeq \frac{N_2 K_{2m} N_e(t)}{\beta + \rho_m}, \tag{18}$$

provided

$$t > (1/\beta)\ln(1 + \beta/\rho_m). \tag{19}$$

In many instances this is more restrictive a condition than necessary. Further discussion of this will be provided later. If Eq. (18) is used in Eq. (6) to eliminate N_m we arrive at a simple form of the ionization equation,

$$dN_e/dt = S + IN_e + BN_e^2, \tag{20}$$

where we have introduced

$$S \equiv N_2[\sigma_{2c}^{(2)} F^2 + \tfrac{1}{2} N_2 v(\sigma_A + \sigma_L F)] \tag{21}$$

as the seed-ionization rate,

$$I \equiv N_2\left(K_{2c} + \sum_{m \geq 3} \frac{K_{2m} P_m}{(\beta + \rho_m)}\right) \tag{22}$$

as the intermediate ionization-rate coefficient, and

$$B \equiv N_2 \sum_{m \geq 3} \frac{K_{2m} K_{mc}}{(\beta + \rho_m)} \tag{23}$$

as the burnout-ionization-rate coefficient.

We see that we can now define

$$N_e^{**} \equiv I/B \tag{24}$$

as the critical electron density at which the burnout rate of ionization equals the intermediate rate of ionization. In a like manner we can also define

$$N_e^{*} \equiv S/I \tag{25}$$

as the characteristic electron density for which the intermediate ionization rate equals the seed-ionization rate. It is apparent from a comparison of Eq. (16) with Eq. (20) that we can identify β with I and N_{e0} with N_e^*. In which case we can write

$$I = N_2\left(K_{2c} + \sum_{m \geq 3} \frac{K_{2m} P_m}{(I + \rho_m)}\right) \tag{26}$$

and

$$B = N_2 \sum_{m \geq 3} \frac{K_{2c} K_{mc}}{(I + \rho_m)}. \tag{27}$$

I can be evaluated in an iterative manner by substituting $\rho_m = \rho_{max} \equiv \rho$ into Eq. (26) and obtaining a first approximation of the form

$$I \simeq \tfrac{1}{2}(\kappa - \rho) + \tfrac{1}{2}\left[(\kappa - \rho)^2 + 4\left(\kappa\rho + N_2 \sum_{m \geq 3} K_{2m} P_m\right)\right]^{1/2}, \tag{28}$$

where $\kappa \equiv N_2 K_{2c}$. If this first approximation is then reintroduced into the right-hand side of Eq. (26), we have found that in almost all cases I is within 1% of the correct (limiting) value.

The simple-model LIBORS ionization [Eq. (20)] has two forms of analytical solution depending upon the relative values of S, I, and B. If $I^2 < 4SB$, which is equivalent to $N_e^{**} < N_e^*$, then ionization proceeds directly from stage 2 to stage 4—that is to say, seed ionization leads directly to runaway ionization. The solution to Eq. (20) under these circumstances takes the form

$$t = \frac{2}{a}\left[\tan^{-1}\left(\frac{2BN_e + I}{a}\right) - \tan^{-1}\left(\frac{I}{a}\right)\right], \tag{29}$$

where

$$a \equiv (4SB - I^2)^{1/2} \tag{30}$$

This class of solution is indicative of a very high rate of seed ionization and we shall refer to this as an S3 solution.

If $I^2 > 4SB$, which is equivalent to $N_e^{**} > N_e^*$, stage 3 ionization will play some role in separating stage 2 from stage 4—that is to say intermediate ionization is significant in increasing the free-electron density to the point where runaway ionization occurs. The solution of the ionization Eq. (20) under these circumstances takes the form

$$t = \frac{1}{A}\ln\left[\left(\frac{N_e + R_1}{N_e + R_2}\right)\frac{R_2}{R_1}\right], \tag{31}$$

where

$$A \equiv (I^2 - 4SB)^{1/2}, \tag{32}$$

$$R_1 \equiv \left(\frac{I-A}{2B}\right), \tag{33}$$

$$R_2 \equiv \left(\frac{I+A}{2B}\right). \tag{34}$$

If, however, $I^2 \gg 4SB$ (i.e., $N_e^{**} \gg N_e^*$), then the intermediate processes play a major role in determining the ionization burnout time τ_B. We shall discriminate between solutions that arise when $100SB \geq I^2 \geq 4SB$ and those that apply when $I^2 > 100SB$, by designating the former as S2 solutions and the latter as S1 solutions.

The ionization burnout time for $I^2 > 4SB$ solutions takes the form

$$\tau_B = \frac{1}{A} \ln\left[\left(\frac{N_0+R_1}{N_0+R_2}\right)\frac{R_2}{R_1}\right]. \tag{35}$$

However, for S1 solutions, where $I^2 > 100SB$ (or $N_e^{**} > 100N_e^*$) we can approximate this by the expression

$$\tau_B \simeq \frac{1}{I} \ln\left(\frac{N_e^{**}}{N_e^*}\right). \tag{36}$$

This relation lends itself to the pictorial interpretation presented as Fig. 2.

For intermediate levels having zero single-photon ionization cross section at the laser wavelength, we have used the minimum photoionization cross section in Eq. (18) since collision coupling between adjacent levels plays a role, as stated earlier, in equilibrating adjacent levels. We have also found that in some instances, particularly S3 solutions, Eq. (18) grossly overestimates the intermediate-level populations at times corresponding to $\tau_B/3$, as seen from a comparison of N_m obtained by Eqs. (17) and (18). Under these circumstances we have assumed that the intermediate-level populations do not contribute to the intermediate ionization stage and reassign $I = N_2 K_{2c}$.

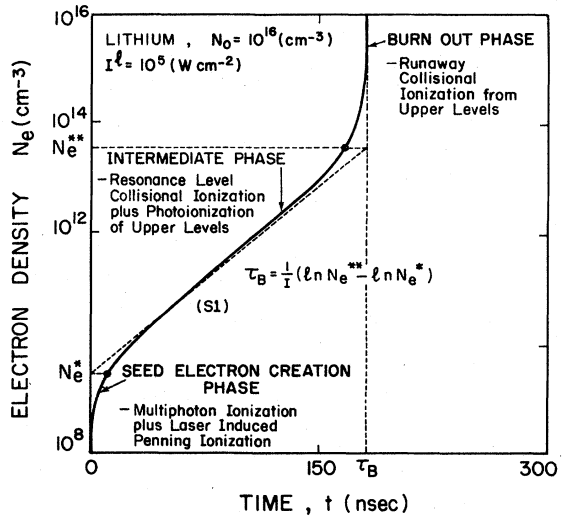

FIG. 2. The three distinct phases (stages 2 to 4 of Fig. 1) of laser ionization based on resonance saturation are indicated in this graph of electron density against time.

In the limit of $I^2 \ll 4SB$, the ionization burnout time

$$\tau_B \simeq \frac{\pi}{2\sqrt{SB}}. \tag{37}$$

LIBORS SIMPLE-MODEL RESULTS FOR ALKALI METALS

In this section we present some representative results of the LIBORS simple-model calculations. The relevant cross sections and parameters required for this analysis are presented for each of the alkali metals in Table I. The type of solution obtained and the appropriate ionization burnout time for each element are also displayed under a wide range of densities and values of laser irradiance. A clear pattern is readily discernible. In the case of lithium all solutions are of the S1 type, which means that the intermediate processes are always important—at least for $10^{15} \leq N_0 \leq 10^{17}$ (cm^{-3}) and $10^5 \leq I^l \leq 10^8$ ($W\,cm^{-2}$) ranges under consideration. S1 solutions are interpreted to mean that the intermediate processes play a dominant role and this appears to be particularly true where associative ionization is absent. The predicted high value of T_e^s is also important.

S1 solutions are also found for sodium under most of these conditions. Reference to Table I shows that for sodium, T_e^s is slightly higher and σ_A is slightly lower than for the remaining alkali metals (*viz.*, K, Rb, and Cs).

At the other end of the periodic table, cesium has predominantly S3 solutions. This is not surprising in light of the predicted low value of T_e^s and relatively high value of σ_A. It is also apparent that potassium and rubidium have S3 solutions at the highest laser powers. In the case of rubidium this can be understood in terms of the high cross sections for both two-photon resonance ionization and laser-induced Penning ionization.

A representative set of ionization curves is presented in Fig. 3. The original density was assumed to be 10^{16} (cm^{-3}) for each of the elements and the laser irradiance was taken as 10^6 ($W\,cm^{-2}$). It is interesting to note that the predicted ionization burnout times for both lithium and sodium are shorter than for potassium and cesium, even though the seed-ionization rates for potassium and cesium are greater. This illustrates that a strong intermediate ionization process can compensate for a lower seed-ionization rate.

TABLE I. Basic parameters, ionization times, and types of LIBORS solutions for alkali metals.[a] S1: $I^2 > 100BS$, S2: $I^2 \gtrsim 4BS$, and S3: $I^2 < 4BS$.

	Li	Na	K	Rb	Cs
E_{21} (eV)	1.85	2.10	1.62	1.58	1.43
T_e^s (K)	11442	8433	7757	8036	4163
σ_A (cm^2)	0	3.26×10^{-18}	1.27×10^{-17}	1.22×10^{-17}	2.19×10^{-17}
(at $N_0=10^{16}$)					
σ_L (cm^4 sec)	9.1×10^{-44}	2.0×10^{-44}	1.2×10^{-43}	9.6×10^{-43}	4.5×10^{-42}
$\sigma_{2c}^{(2)}$ (cm^4 sec)	2.2×10^{-48}	1.7×10^{-49}	2.9×10^{-49}	7.7×10^{-48}	5.8×10^{-48}
$\sigma_{max}^{(1)}$ (cm^2)	1.0×10^{-17}	2.9×10^{-18}	2.3×10^{-18}	8.2×10^{-19}	4.5×10^{-19}
$\langle A_{m2}\rangle$[b] (sec^{-1})	3.5×10^{7}	2.4×10^{7}	2.9×10^{7}	9.8×10^{6}	9.8×10^{6}
$\langle K_{mc}\rangle$ ($cm^3\,sec^{-1}$)	2.5×10^{-7}	1.78×10^{-7}	1.5×10^{-7}	1.6×10^{-7}	3.4×10^{-8}
$\langle K_{2m}\rangle$ (cm^3 sec^{-1})	1.73×10^{-8}	3.62×10^{-8}	8.3×10^{-8}	1.26×10^{-7}	1.42×10^{-7}
N_0 (cm^{-3}) / I^1 ($W\,cm^{-2}$)	Ionization time, τ_B (nsec), and class of solution				
10^{15} / 10^5	1060 (S1)	837 (S1)	994 (S2)	976 (S2)	2740 (S3)
10^{15} / 10^6	479 (S1)	435 (S1)	905 (S2)	762 (S2)	1940 (S2)
10^{15} / 10^7	251 (S1)	204 (S1)	595 (S2)	222 (S3)	294 (S3)
10^{15} / 10^8	124 (S1)	93.0 (S1)	131 (S3)	27.2 (S3)	31.8 (S3)
10^{16} / 10^5	180 (S1)	124 (S1)	92.3 (S2)	87.3 (S2)	171 (S3)
10^{16} / 10^6	84.7 (S1)	80.3 (S1)	91.3 (S2)	81.4 (S2)	138 (S3)
10^{16} / 10^7	38.4 (S1)	41.3 (S1)	82.1 (S2)	44.4 (S3)	55.7 (S3)
10^{16} / 10^8	18.8 (S1)	17.0 (S1)	32.5 (S3)	8.04 (S3)	9.29 (S3)
10^{17} / 10^5	23.2 (S1)	13.9 (S2)	8.56 (S2)	7.63 (S2)	10.6 (S3)
10^{17} / 10^6	13.6 (S1)	11.8 (S2)	8.46 (S2)	7.30 (S2)	9.42 (S3)
10^{17} / 10^7	6.39 (S1)	7.63 (S1)	7.83 (S2)	5.46 (S2)	5.50 (S3)
10^{17} / 10^8	2.84 (S1)	3.60 (S1)	4.88 (S3)	1.89 (S3)	1.78 (S3)

[a] The "intermediate levels" used correspond to the next four levels that are optically connected to the resonance level.

[b] The results presented in this table assume radiation trapping with a scale length of 0.1 cm.

In Fig. 4 we plot the variation of the ionization burnout time against the laser irradiance for an initial atom density of 10^{16} cm^{-3} for all of the alkali metals considered (Li through to Cs). It is clear that in the case of potassium, rubidium, and cesium, the laser dependence of the ionization burnout time τ_B is weak at the lower values of laser irradiance. This can be understood in terms of the dominance of associative ionization. Then at the higher values of laser irradiance the influence of laser-induced Penning ionization (and to a lesser extent two-photon ionization) becomes apparent by the rapid fall in τ_B with I^1.

On the other hand, the variation of τ_B with I^1 for lithium and sodium can be seen to be much more consistent. This is reasonable in light of the fact that both these elements have lower values of σ_A and σ_L and are controlled much more by the intermediate stage of ionization. In Fig. 5 we have plotted the variation of the ionization burnout time against the initial atom density at a given laser irradiance of 10^6 ($W\,cm^{-2}$) for each of the alkali metals. From this figure it is clear that full ionization is expected for both lithium and sodium under the experimental conditions of the work by Lucatorto and McIlrath.[1,2] They operated with a laser-pulse duration of about 500 nsec, a peak irradiance of about 10^6 ($W\,cm^{-2}$) and densities 6×10^{15} (cm^{-3}) and 10^{16} (cm^{-3}) for lithium and sodium, respectively. On the other hand, appreciable

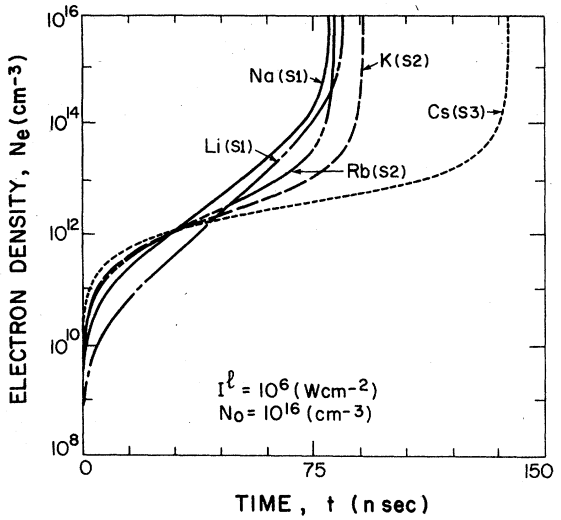

FIG. 3. Ionization time histories for each of the alkali metals as predicted by the LIBORS simple model. The initial number density, $N_0 = 10^{16}$ cm^{-3}, and the laser irradiance $I^{\ell} = 10^{6}$ W cm^{-2}.

ionization would not be expected under the experimental conditions of Salter *et al.*[23]

The ionization times predicted in Table I assume that radiation trapping is present and corresponds to a saturating laser-beam radius of 0.1 cm.

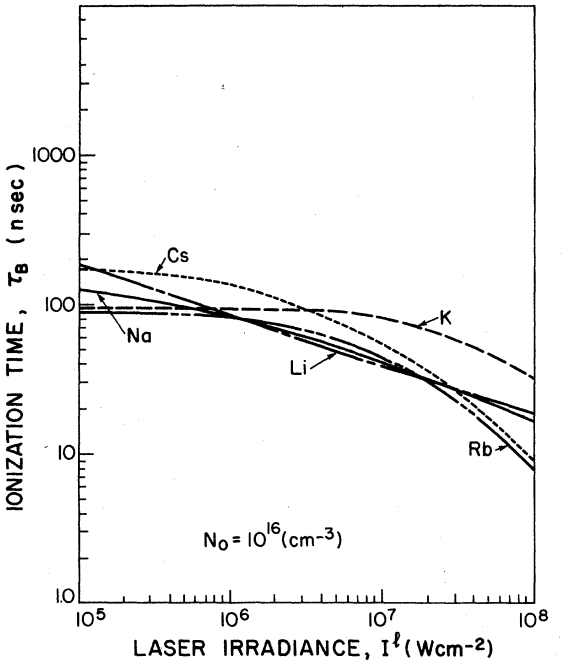

FIG. 4. The variation of the ionization burnout time τ_B, with laser irradiance for each of the alkali metals at an initial density of 10^{16} cm^{-3} as predicted by the LIBORS simple model.

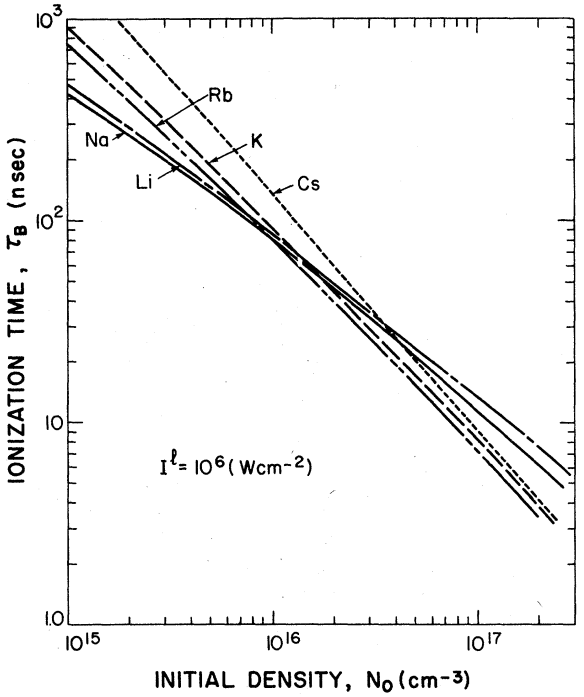

FIG. 5. The variation of the ionization burnout time τ_B, with initial density at a laser irradiance of 10^{6} W cm^{-2} for each of the alkali metals as predicted by the LIBORS simple model.

Although this is quite reasonable, we have considered the influence of neglecting radiation trapping. As might be expected the importance of radiation trapping is less pronounced at high values of density and laser irradiance. This can be seen by reference to Table II, where the ionization times are recalculated assuming "no radiation trapping". The differences in the ionization curves *with* and *without radiation trapping* are illustrated for sodium at an initial density of 10^{16} (cm^{-3}) in Fig. 6.

Although we have attempted to take account of all of the important collisional-radiative processes, ionization resulting from the collision of two excited atoms, where one is in the resonance state and the other is in an intermediate state has not been included in the work presented in this paper. Such collisions could have a large cross section[33,34] and could be fitted into our model, increasing the intermediate ionization-rate coefficient I, and slightly decreasing the burnout rate coefficient B. Our reason for not including them at this time lies in a lack of reliable cross-section data.

Nevertheless, we have undertaken a preliminary parametric study using a range of possible cross sections in the case of cesium. Our results suggest that the ionization time could be considerably

TABLE II. Ionization times (nsec) and types of LIBORS solution for each of the alkali metals assuming no radiation trapping.

N_0 (cm^{-3})	I^l (Wcm^{-2})	Li	Na	K	Rb	Cs
10^{15}	10^5	2430 (S1)	1970 (S1)	1720 (S1)	1240 (S1)	6440 (S3)
10^{15}	10^6	809 (S1)	755 (S1)	1670 (S1)	985 (S1)	3340 (S2)
10^{15}	10^7	288 (S1)	250 (S1)	1160 (S2)	342 (S2)	764 (S3)
10^{15}	10^8	131 (S1)	97.2 (S1)	300 (S3)	50.3 (S3)	82.8 (S3)
10^{16}	10^5	229 (S1)	159 (S1)	112 (S2)	92.0 (S2)	255 (S3)
10^{16}	10^6	101 (S1)	94.3 (S1)	110 (S2)	85.5 (S2)	196 (S3)
10^{16}	10^7	40.7 (S1)	44.0 (S1)	94.3 (S2)	48.3 (S2)	75.9 (S3)
10^{16}	10^8	18.9 (S1)	17.5 (S1)	41.5 (S3)	9.00 (S3)	12.7 (S3)
10^{17}	10^5	24.0 (S1)	14.6 (S2)	8.77 (S2)	7.65 (S2)	12.2 (S3)
10^{17}	10^6	14.0 (S2)	12.2 (S2)	8.70 (S2)	7.35 (S2)	10.8 (S3)
10^{17}	10^7	6.49 (S1)	7.75 (S1)	8.09 (S2)	5.52 (S2)	6.11 (S3)
10^{17}	10^8	2.86 (S1)	3.64 (S1)	5.05 (S3)	1.92 (S3)	1.96 (S3)

shorter than we currently predict for cross sections of about 10^{-14} (cm^2) and under these circumstances most of the ionization curves switch from S3 to S1 solutions.

SIMPLE-MODEL COMPARISON WITH LIBORS COMPUTER-CODE RESULTS

As a further check on the reliability of our simple model of LIBORS, we have compared the ionization burnout times predicted by the simple model with that of our extensive computer code.[15-18] This comparison has, at the moment, been restricted to sodium due to the cost and time involved in running the code for a different alkali. The results, as evident in Fig. 7, are very encouraging for they indicate that over the range of densities and laser irradiances of interest in the present work excellent agreement ($\lesssim$15%) is obtained. Furthermore, there is also excellent agreement in the detailed features of the ionization time histories. This can be gauged by comparing the N_e curve in Fig. 8 with the corresponding ionization curve for sodium in Fig. 6. Both display the same shape and have changes of slope at about the same values of N_e.

It is also worth pointing out that the LIBORS computer-code results, as shown in Fig. 8, confirm that our basic assumptions regarding the constancy of N_2 and T_e over the major portion of

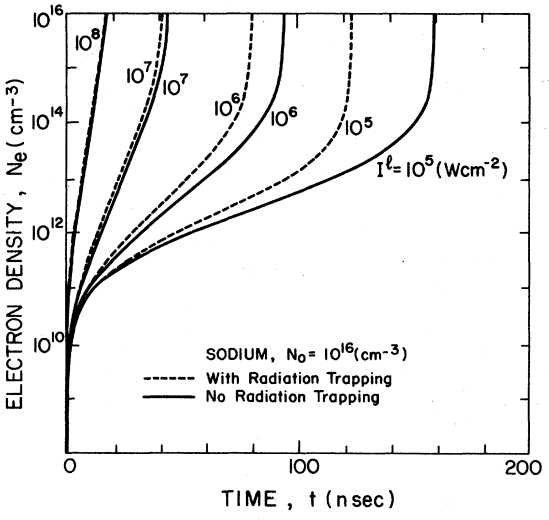

FIG. 6. Ionization curves for sodium *with* and *without* radiation trapping, as predicted by the LIBORS simple model.

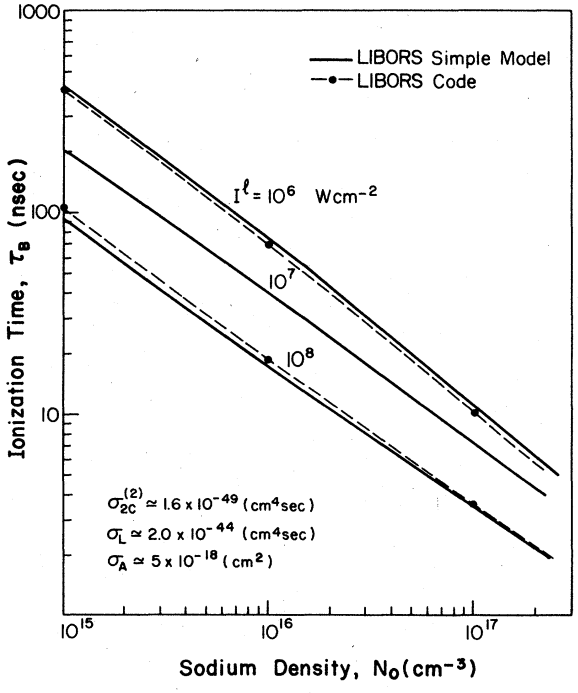

FIG. 7. A comparison of the ionization burnout time ($\simeq$95%) variation with density as predicted by the LIBORS simple model and the full computer code for sodium. Radiation trapping assumed for both with scale length of 0.1 cm.

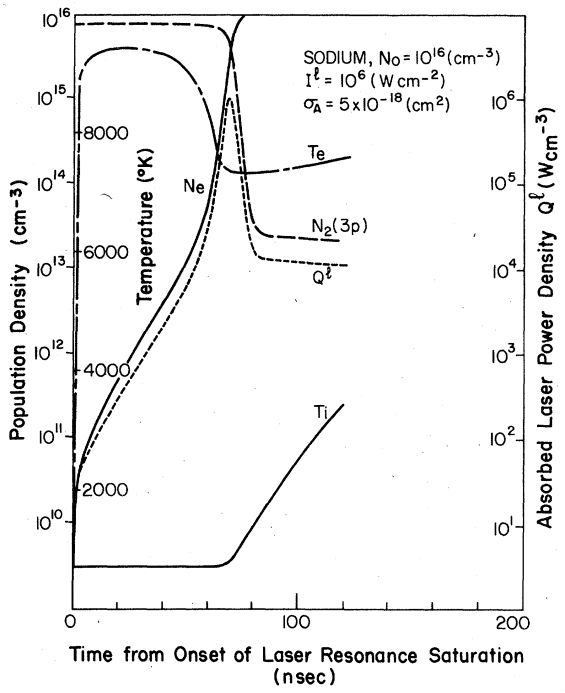

FIG. 8. Time histories of N_e, T_e, N_2, Q^l and T_i as predicted by the full LIBORS computer code (Refs. 15 to 18) for sodium with an original density of 10^{16} cm^{-3} and a laser irradiance $I^l = 10^6$ W cm^{-2}.

the ionization time are reasonable. Not shown, but in fact observed in our LIBORS code results is the proportionality of the intermediate-state population densities and the electron density over much of the ionization period—corresponding to Eq. (18).

CONCLUSIONS

We have developed a relatively simple model of laser ionization based on resonance saturation. This model includes essentially all of the important collisional and radiative interactions that come into play when an alkali metal vapor (density range 10^{15} to 10^{17} cm^{-3}) is subject to a sudden pulse of intense laser radiation that is tuned to one of the resonance transitions of the alkali atom. This model reveals that once laser saturation of the relevant resonance transition has been achieved, ionization proceeds in three stages: First, seed ionization (including associative, laser-induced Penning and multiphoton ionization) creates an initial pool of seed electrons. Subsequently, in the intermediate ionization phase these free electrons are heated through superelastic collisions and then populate intermediate energy states which in turn are photoionized by the laser radiation. Finally, runaway ionization, through direct electron-impact ionization of the intermediate-level population, leads to a very rapid and near complete ionization burnout of the laser-irradiated species.

We have also been able to show that this model leads to two types of analytical solutions for the ionization time history of the irradiated vapor. Physical interpretation of the conditions that mediate which type of analytical solution characterizes the ionization time history is also provided. The ionization time for each of the alkali metals (Li through to Cs) has been evaluated under a wide range of conditions: initial number densities 10^{15} to 10^{17} cm^{-3} and laser irradiances from 10^5 to 10^8 W cm^{-2}. Although to date there has been very limited experimental work on this new class of dense plasma production, where results have been available they are consistent with our predictions. We have also been able to show that the predicted ionization times of this model are in excellent agreement with the results of our comprehensive LIBORS computer code, over a wide range of densities and laser irradiances, in the case of sodium. In general, the predictions of our simple LIBORS model should only be regarded as a guide to the expected time to achieve ionization burnout since the spatial and temporal characteristics of the laser beam will not in reality be rectangular and because many of the cross sections used are not known with great precision. Furthermore, our neglect of continuity is not valid for electron densities $\gtrsim 10\%$, and this leads to an underestimate of the full ($> 95\%$) ionization time by about 25% for all but S3 solutions. A more detailed analysis of this will shortly be published by us.[35]

ACKNOWLEDGMENTS

Work supported by the Air Force Office of Scientific Research (AFOSR) (under Grant No. 76-2902C) and the Natural Science and Energy Research Council of Canada. Scholarship support for P. G. Cardinal was provided by the Natural Science and Engineering Research Council of Canada.

[1]T. B. Lucatorto and T. J. McIlrath, Phys. Rev. Lett. 37, 428 (1976).
[2]T. J. McIlrath and T. B. Lucatorto, Phys. Rev. Lett. 38, 1390 (1977).
[3]C. H. Skinner, J. Phys. B 13, 55 (1980).
[4]W. A. Young, M. Y. Mirza, and W. W. Duley, Opt. Commun. 31, 157 (1979).
[5]S. G. Leslie, J. T. Verdeyen, and W. S. Millar, J. Appl.

Phys. 48, 4444 (1977).
[6]A. C. Tam and W. Happer, Opt. Commun. 21, 403 (1977).
[7]G. H. Bearman and J. J. Leventhal, Phys. Rev. Lett. 41, 1227 (1978).
[8]M. Allegrini, G. Alzetta, A. Kopystynska, L. Moi, and G. Orriols, Opt. Commun. 22, 329 (1977).
[9]S. Geltman, J. Phys. B 10, 3057 (1977).
[10]R. M. Measures, J. Quant. Spectrosc. Radiat. Transfer 10, 107 (1970).
[11]R. M. Measures, J. Appl. Phys. 48, 2673 (1977).
[12]A. de Jong and F. van der Valk, J. Phys. B 12, L561 (1979).
[13]E. F. Worden, J. A. Paisner, and J. G. Conway, Opt. Lett. 3, 156 (1978).
[14]A. Klucharev, V. Sepman, and V. Vujnovic, J. Phys. B. 10, 715 (1977).
[15]P. G. Cardinal, UTIAS M.A.Sc. thesis, 1979 (unpublished).
[16]N. Drewell, UTIAS Report No. 229, 1979.
[17]R. M. Measures, N. Drewell, and P. Cardinal, J. Appl. Phys. 50, 2662 (1979).
[18]R. M. Measures, N. Drewell, and P. Cardinal, Appl. Opt. 18, 1824 (1979).
[19]R. M. Measures, P. L. Wizinowich, and P. G. Cardinal, J. Appl. Phys. 51, 3622 (1980).
[20]D. P. Burgess and M. J. Eckart, J. Phys. B 9, L519 (1976).
[21]B. L. Sharp and A. Goldwasser, Spectrochim. Acta, Part B 31, 431 (1976).
[22]J. M. Salter, J. Phys. B 12, L763 (1979).
[23]R. M. Measures, J. Appl. Phys. 39, 5232 (1968).
[24]J. M. Salter, D. D. Burgess, and N. A. Ebrahim, J. Phys. B 12, L759 (1979).
[25]A. B. Rodrigo and R. M. Measures, IEEE J. Quantum. Electron. QE-9, 972 (1973).
[26]J. W. Daily, Appl. Opt. 17, 225 (1978).
[27]G. S. Hurst, M. G. Payne, S. D. Kramer, and J. P. Young, Rev. Mod. Phys. 51, 767 (1979).
[28]T. J. McIlrath and J. L. Carlsten, Phys. Rev. A 6, 1091 (1972).
[29]Although the normal electron-electron relaxation time would suggest that at early time, deviations from a Maxwellian distribution might be appreciable, the very short time associated with inelastic collisional processes at the high density of atoms could well justify the assumption of a Maxwellian velocity distribution for times where $N_e > N_e^*$. For times less than this, the intermediate ionization (which is T_e dependent) is not regarded as important.
[30]G. V. Marr, *Photoionization Processes in Gases* (Academic, New York, 1967).
[31]M. J. Seaton, *Atomic and Molecular Processes*, edited by D. R. Bates (Academic, New York, 1962).
[32]T. Holstein, Phys. Rev. 83, 1159 (1951).
[33]R. E. Olson, J. Phys. B 12, L109 (1979).
[34]A. N. Klyucharev, A. V. Lazarenko, and V. A. Sheverev, Opt. Spektrosk. 46, 1157 (1979) [Opt. Spectrosc. (USSR) 46, 653 (1979)].
[35]R. M. Measures, P. G. Cardinal, and G. W. Schinn, J. Appl. Phys. (to be published).